Molecular Crystals and Liquid Crystals
Publication details, including instructions for authors and subscription information:
http://www.tandfonline.com/loi/gmcl16

Resonance Spectra of a Paramagnetic Probe Dissolved in a Viscous Medium

Jerome I. Kaplan [a] , Edward Gelerinter [b] & George C. Fryburg [c]

[a] Battelle Memorial Insitute, Columbus, Ohio, 43201

[b] Physics Department and Liquid Crystal, Institute Kent State University, Kent, Ohio, 44242

[c] NASA Lewis Research Center, Cleveland, Ohio, 44135

Version of record first published: 21 Mar 2007.

To cite this article: Jerome I. Kaplan , Edward Gelerinter & George C. Fryburg (1973): Resonance Spectra of a Paramagnetic Probe Dissolved in a Viscous Medium, Molecular Crystals and Liquid Crystals, 23:1-2, 69-83

To link to this article: http://dx.doi.org/10.1080/15421407308083362

Molecular Crystals and Liquid Crystals. 1973. Vol. 23, pp. 69–83

Resonance Spectra of a Paramagnetic Probe Dissolved in a Viscous Medium

JEROME I. KAPLAN

Battelle Memorial Institute
Columbus, Ohio 43201

EDWARD GELERINTER

Physics Department and Liquid Crystal Institute
Kent State University
Kent, Ohio 44242

and

GEORGE C. FRYBURG

NASA Lewis Research Center
Cleveland, Ohio 44135

Received October 12, 1972; *in final form December* 4, 1972

Abstract—A model is presented in which one calculates the paramagnetic resonance (EPR) spectrum of vanadyl acetylacetonate (VAAC) dissolved in either a liquid crystal or isotropic solvent. It employs density matrix formulation in the rotating reference frame. The molecules occupy several discrete angles with respect to the magnetic field and can relax to neighboring positions in a characteristic time $\tau(\theta)$. The form of $\tau(\theta)$ is found from a diffusion approach, and the magnitude of $\tau(\theta)$ is a measure of how freely the VAAC probe tumbles in the solvent. Spectra are predicted for values of τ between 10^{-11} sec and 10^{-7} sec. The EPR spectrum, in the isotropic case, is obtained by summing the contributions from the allowed angles weighted by the polar volume element, $\sin\theta$. When applying the model to the nematic liquid crystal case it is also necessary to multiply by the Saupe distribution function. For this case, $\tau(\theta)$ is obtained from the diffusion approach in which two diffusion constants are employed to reflect the difference in the parallel and perpendicular components of the viscosity.

Electron paramagnetic resonance (EPR) has been used to measure the ordering of the probe molecule vanadyl acetylacetonate (VAAC) ($I = 7/2$ $S = 1/2$) when dissolved in liquid crystal media.[1–4] These media inhibit the tumbling of the probe molecule to various extents depending upon the temperature and solvent material. If the probe is not completely free to tumble, then the EPR spectra will be affected. The assumption that the spatial and temporal averages

are equal breaks down, and the EPR data must be interpreted in this light. The end cases of extremely fast and slow tumbling have been discussed in the literature[3,4] and are well understood. The intermediate case is more difficult, however. Other authors[5,6] have successfully dealt with the intermediate case for isotropic liquids. The model which we are presenting is easily adapted to both nematic liquid crystal and isotropic solvents. The technique is also easier to deal with from a computational point of view.

In this model the molecules are assigned a discrete number of allowed angular positions. These positions are described by angles θ_1, θ_2, etc. measured from the preferred direction in the case of a liquid crystal solvent and from the polar axis for the case of an isotropic liquid. Both axes correspond to the direction of applied magnetic field. A molecule in the θ_n position can only relax to the θ_{n-1} or the θ_{n+1} position with a characteristic time $\tau(\theta)$. The choices of θ's and τ's are described below. The starting Hamiltonian in laboratory coordinates is given by[4]

$$\mathcal{H} = g\beta H_z S_z + aI \cdot S + 1/3(\Delta g \beta H_z + bI_z)(3\cos^2\theta - 1)S_z - b/12(3\cos^2\theta - 1)(S_+ I_- + S_- I_+) \quad (1)$$

where g, a and Δg, b are the isotropic and anisotropic portions of the "g" and hyperfine tensors, respectively. S and I refer to the electronic and nuclear spin operators. Equation (1) can be rewritten as

$$\mathcal{H} = \alpha S_z + A(\theta) I_z S_z + a/2(S_+ I_- + S_- I_+) - B(\theta)(S_+ I_- + S_- I_+) \quad (2)$$

where

$$\alpha = \left[1 + \frac{1}{3}\frac{\Delta g}{g}(3\cos^2\theta - 1)\right] g\beta H_z,$$

$$B(\theta) = b/12(3\cos^2\theta - 1)$$

and

$$A(\theta) = a + \tfrac{1}{3}b(3\cos^2\theta - 1).$$

An rf field is applied

$$H_1 = \omega_1(S_x \cos\omega t - S_y \sin\omega t). \quad (3)$$

Using the density matrix notation in the rotating frame we have

$$\dot{\rho}_r = -i\hbar^{-1}[\mathcal{H}_r(\theta), \rho_r], \quad (4)$$

where

$$\mathcal{H}_r = \mathcal{H}_0 + \mathcal{H}_1, \quad (5)$$

and

$$\mathscr{H}_0 \equiv (\alpha-\omega)S_z + A(\theta)S_z I_z - \omega I_z + a/2(S_+ I_- + S_- I_+) - B(\theta)(S_+ I_- + S_- I_+),$$

$$\mathscr{H}_1 \equiv \omega_1 S_x.$$

Let $\rho_r = \rho_0 + \rho_1$, where ρ_0 is zero order in ω_1 and ρ_1 is linear in ω_1. In addition for a steady state solution $\dot{\rho}_r = 0$. Substituting into (4) and retaining terms up to first order in ω_1

$$0 = -i\hbar^{-1}[\mathscr{H}_0(\theta), \rho_1] - i\hbar^{-1}[\mathscr{H}_1, \rho_0]. \tag{7}$$

In addition to (7) a term of the form $-\rho_1(\theta)/T_2$ must be included to represent relaxation of the molecule due to random perturbations and a term, $-1/\tau(\theta)$, to represent relaxation to other angles. The form of $\tau(\theta)$ is obtained using a diffusion approach. We start with

$$\nabla^2 V = D_1\left(\frac{\partial^2 V}{\partial x^2} + \frac{\partial^2 V}{\partial y^2}\right) + D_2 \frac{\partial^2 V}{\partial z^2}. \tag{8}$$

Here D_2 and D_1 are the parallel and perpendicular diffusion constants, respectively. The θ component of $\nabla^2 V$ is obtained, after some calculation, as

$$\frac{1}{\tau}\left[2V(\theta_i)\left\{1 + \frac{D_2 - D_1}{D_1}\sin^2\theta_1\right\} - V(\theta_{i+1})\left\{1 + \frac{D_2 - D_1}{D_1}\sin^2\theta_i + \Delta\cot\theta_i + \frac{\Delta}{2}\frac{D_2 - D_1}{D_1}\sin 2\theta_i\right\} - V(\theta_{i-1})\left\{1 + \frac{D_2 - D_1}{D_1}\sin^2\theta_i - \frac{\Delta}{2}\cot\theta_i - \frac{\Delta}{2}\frac{D_2 - D_1}{D_1}\sin 2\theta_i\right\}\right], \tag{9}$$

where $1/\tau = D_1^2/r^2\Delta^2$. Here $\Delta = \theta_{i+1} - \theta_i$ and the derivatives are calculated by the finite difference method, as

$$\frac{\partial V}{\partial \theta} = \frac{V(\theta_{i+1}) - V(\theta_{i-1})}{2\Delta}, \tag{10}$$

and

$$\frac{\partial^2 V}{\partial \theta^2} = \frac{V(\theta_{i+1}) - 2V(\theta_i) + V(\theta_{i-1})}{\Delta^2}.$$

The form of the relaxation time is obtained using the form of Eq. (9).

Equation (7) is now modified to become, for the i^{th} position,

$$0 = -i\hbar^{-1}[\mathscr{H}_0(\theta_i), \rho_1(\theta_i)] - i\hbar^{-1}[\mathscr{H}_1(\theta_i), \rho_0(\theta_i)] - \frac{\rho_1(\theta_i)}{T_2}$$
$$-\frac{1}{\tau}\left[2\rho(\theta_i)\left\{1+\frac{D_2-D_1}{D_1}\sin^2\theta_1\right\} - \rho(\theta_{i+1})\left\{1+\frac{D_2-D_1}{D_1}\sin^2\theta_i\right.\right.$$
$$\left.+\frac{\Delta}{2}\cot\theta_i+\frac{\Delta}{2}\frac{D_2-D_1}{D_1}\sin 2\theta_i\right\} - \rho(\theta_{i-1})\left\{1+\frac{D_2-D_1}{D_1}\sin^2\theta_i\right.$$
$$\left.\left.-\frac{\Delta}{2}\cot\theta_i-\frac{\Delta}{2}\frac{D_2-D_1}{D_1}\sin 2\theta_i\right\}\right]\frac{1}{\exp(-\beta\cos^2\theta)}. \qquad (11)$$

The last term in Eq. (11) represents the additional concentration dependence of the relaxation rate.

The quantity $K = D_2 - D_1/D_1$ is a measure of the anisotropy of the diffusion constants, e.g., $K = 1$ corresponds to a 2 to 1 anisotropy, and $K = 0$ corresponds to an isotropic liquid. The $\exp(-\beta\cos^2\theta)$ is the Saupe distribution function. The negative sign indicates that the VAAC is aligned perpendicular to the field. $[\mathscr{H}_1, \rho_0]$ can be evaluated as

$$\frac{1}{2}\frac{\omega_1\omega_0}{kT}(S_+ - S_-), \qquad (12)$$

where $\omega_0 = g\beta Hz$.

It is now necessary to choose values of θ_i. In order to avoid computational difficulties, $\theta = 0$, i.e., $\cot\theta = \infty$, will be avoided. We choose $\theta_1 = \pi/34$ and $\Delta = \pi/17$. This gives 9 allowed positions in the first quadrant with $\theta_9 = \pi/2$. Since the Hamiltonian is an even function of θ, $\rho(\theta_i) = \rho(\theta_{-i})$. We have also assumed that the molecules cannot be distinguished end from end and this yields $\rho(\theta_i) = \rho(\pi + \theta_i)$. This makes the four quadrants equivalent so that we will restrict ourselves to the first quadrant. Equation (11) then is really a series of 9 equations corresponding to the 9 allowed positions. The case of slow tumbling ($1/\tau < 20$) requires the use of more positions in order to obtain usable spectra. We used 73 positions in these cases.

The absorption is given as

$$Ab = \int d\Omega T r\rho(\theta) S_y \exp(-\beta\cos^2\theta). \qquad (13)$$

VAAC has a nuclear spin of 7/2, thus its EPR spectrum consists of eight lines. The line corresponding to $m_I = 7/2$ is obtained as

$$\text{absorption} = Im \sum_{\theta_i} < 7/2, 1/2, \left| \rho(\theta_i) \right| 7/2, -1/2 > \sin\theta_i \exp(-\beta \cos^2\theta). \tag{14}$$

The forms for the other values of m_I's are similar. The $m_I = 7/2$'s line is coupled to the $m_I = 5/2$'s line via the I_- operator so that it is necessary to solve an 18×18 matrix to obtain the $< 7/2, 1/2 \left| \rho(\theta_i) \right| 7/2, -1/2 >$ elements. A 36×36 matrix is required for all of the other lines, except $m_I = -7/2$, since these lines couple to the higher and lower hyperfine lines via the $I_\pm$ operators.

In this treatment, τ is varied from approximately 10^{-12} sec for the fast tumbling case to approximately 10^{-7} sec for the slow tumbling case. T_2 is a measure of the inherent line width; i.e., the line width when τ is small. It was obtained from the experimental line widths reported by Wilson and Kivelson[6] for $\sim 10^{-4}$ M VAAC in benzene, at room temperature. T_2 is different for each line and has been assumed constant with respect to τ for the purpose of these calculations. This makes the calculation give the correct line widths for the fast tumbling case. In reality, T_2 varies somewhat with viscosity. However, it is mainly the contribution of τ that determines the line width in the intermediate case, so that keeping T_2 constant is a good approximation. It is also τ that affects the line positions which is the property of interest in calculating the order in the liquid crystal. The treatment neglects the small effects of the pseudo-secular terms. A method for including these terms is presented in the appendix for the case $K = \beta = 0$, i.e., the isotropic liquid.

The calculated EPR spectra are studied as a function of the relaxation time, τ, the Saupe factor β and the anisotropy in the diffusion constants, K. It is possible to calculate the tumbling rate, $1/\tau$, in Gauss as well as $\sec^{-1}$. This is useful sometimes, in order to facilitate comparison with experimental splittings. The constant β is dimensionless since it is an energy divided by kT. The order σ_z is defined as

$$\frac{1}{2}\int_0^\pi (3\cos^2\theta - 1) \exp(-\beta \cos^2\theta) \sin\theta \, d\theta \Big/ \int^\pi \exp(-\beta \cos^2\theta \sin\theta \, d\theta.$$

The constant K is also dimensionless.

Some typical spectra have been calculated and are shown in Fig. 1. The upper two spectra are for an isotropic liquid, i.e., $K = \beta = 0$. The first spectrum is for the fast tumbling case, $1/\tau = 5.6 \times 10^{10}$ sec^{-1} (20,000 G), and is identical with the experimental spectra obtained in benzene at 298 °K.[6] The second spectrum is for a slightly slower tumbling rate $1/\tau = 1.4 \times 10^{10}$ sec^{-1} (5,000 G) and illustrates the line broadening associated with a small inhibition of the tumbling. It is characteristic of the spectra obtained with a typical liquid crystal in its isotropic phase (Ref. 4, Fig. 3(a)). More pronounced inhibition of the tumbling results in a further increase in line width and even in a large decrease in the overall splitting. This case will be treated in more detail in a future publication.

The lower two spectra are typical of liquid crystals in their nematic phase. For the third spectrum, we have taken $\beta = 3.2$ (corresponding to an order $\sigma_z = -0.29$), $1/\tau = 1.4 \times 10^{10}$ sec^{-1} (5,000 G), and $K = 2$. This spectrum is similar to that of Fig. 3(b), Ref. 4, except the order is slightly larger. One should note the contraction of the hyperfine splitting indicative of the ordering in the liquid crystal phase. As the temperature is lowered, the order increases, the liquid crystal becomes more viscous and the tumbling is further slowed. In the fourth spectrum we illustrate such a case, with $\beta = 3.6$

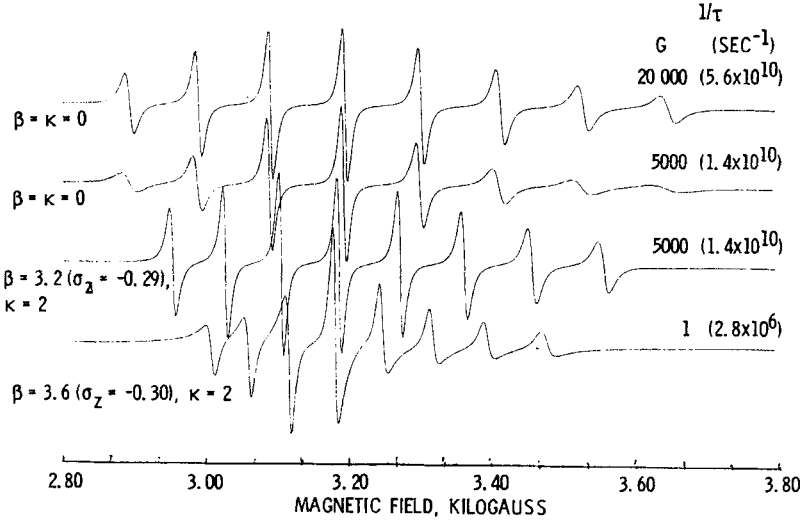

Figure 1. Calculated spectra for some representative isotropic and liquid crystal cases.

($\sigma_z = -0.30$), $1/\tau = 2.8 \times 10^6$ sec^{-1} (1 G) and $K = 2$. This spectrum is similar to that of Fig. 3(c), Ref. 4. Now the splitting is reduced further and one notes some asymmetry in the line shapes. This asymmetry is characteristic of highly inhibited tumbling.

The apparent order in a liquid crystal can be obtained for a spectrum of this last type from the average hyperfine splitting, $\langle a \rangle$, and the formula,

$$\sigma_z(\text{apparent}) = \frac{1}{2}\frac{\langle a \rangle - a}{a - A\perp},$$

where a and $A\perp$ are isotropic and perpendicular components of the hyperfine tensor. This apparent order is a function of both the real order, σ_z, and the tumbling time. In Fig. 2 we show the effect of the real order on the average hyperfine splitting, and in Fig. 3 we show the effect of the tumbling rate.

The decrease in $\langle a \rangle$ resulting from an increase in the real order is shown in Fig. 2 in which we show the $m_I = \pm 7/2$'s line for values of $\beta = 2(\sigma_z = -0.21)$, $3.6(\sigma_z = -0.30)$, $7.5(\sigma_z = -0.41)$ and $15(\sigma_z = -0.45)$. In all of these spectra $K = 2$ and $1/\tau = 1.4 \times 10^{10}$ sec^{-1} (5,000 G). The contraction of the spectra is similar to that observed experimentally as the order in a liquid crystal increases.

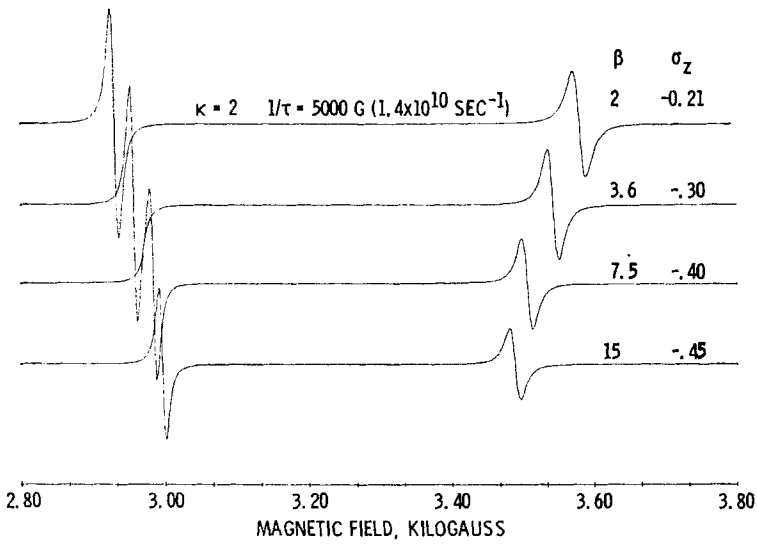

Figure 2. Calculated spectra for different values of the Saupe factor, β.

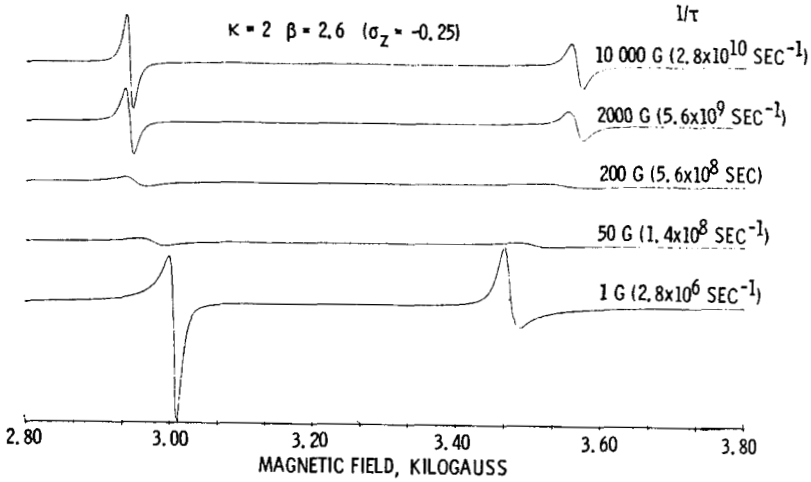

Figure 3. Calculated spectra for different values of the tumbling time.

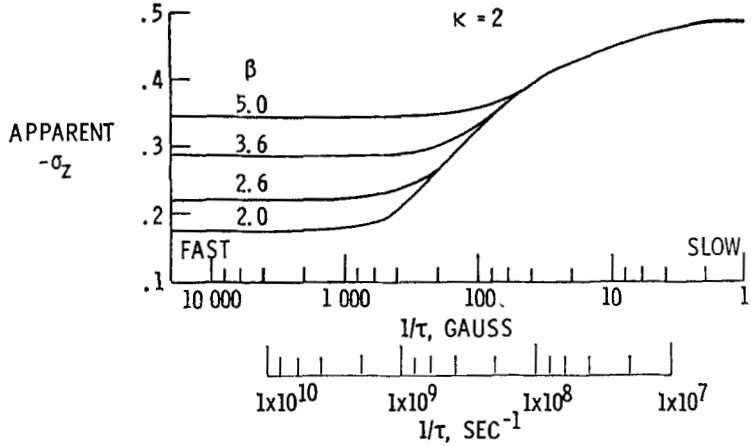

Figure 4. The apparent order, as calculated from the average line separation, versus the tumbling rate, with β as a parameter.

The decrease in $\langle a \rangle$ resulting from a decrease in the tumbling rate is illustrated in Fig. 3. Here the order is constant; $\beta = 2.6(\sigma_z = -0.25)$ and $K = 2$. The spectra are displayed for $1/\tau = 2.8 \times 10^{10}$, 5.6×10^{9}, 5.6×10^{8}, 1.4×10^{8} and 2.8×10^{6} sec^{-1}. The initial effect of slowing the tumbling is to increase the line width. This is followed by a decrease in $\langle a \rangle$ as the tumbling is further reduced. The extreme case of very slow tumbling shows asymmetric lines that are narrowed, and the average separation between the lines corresponds to nearly perfect apparent order (-0.5).

We have investigated the effect of the parameters used in this calculation. The results are shown graphically in the next four figures. In Fig. 4 we have plotted the apparent order, calculated from the average line separations, versus $1/\tau$ for four values of β. In the case of fast tumbling the apparent order is approximately equal to the real order. As the tumbling is slowed, the curves for the different β's coalesce. They all approach perfect order (-0.5) for slow tumbling. The apparent order deviates significantly from the real order when $1/\tau <$ few times the hyperfine splitting.

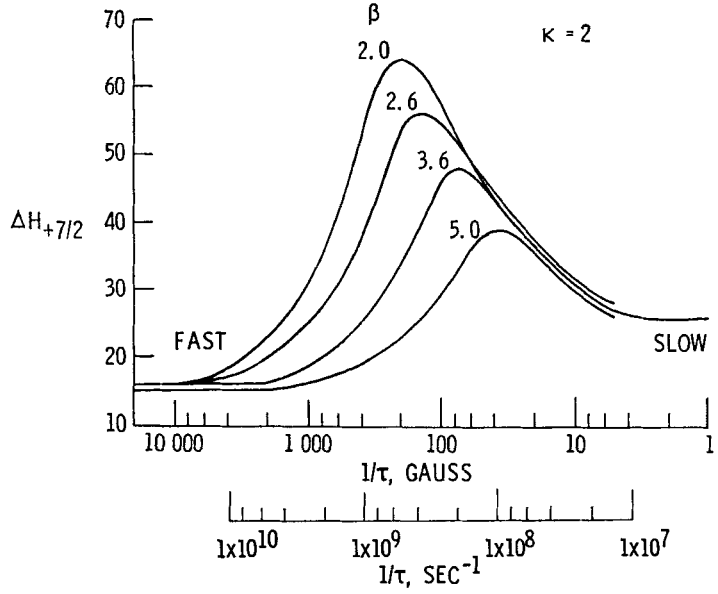

Figure 5. The peak to peak derivative line width of the $m_I = +7/2$ line versus the tumbling rate, with β as a parameter.

In Fig. 5 we show the peak to peak linewidth versus $1/\tau$ for the same four values of β. In all cases the linewidth maximizes at some intermediate value of $1/\tau$. The lower order corresponds to a higher maximum at a lower value of $1/\tau$. The curves coalesce at the extremes of $1/\tau$. The linewidth begins to increase when $1/\tau <$ a few times the Zeeman splitting. The maximum in peak to peak linewidth occurs when $1/\tau \approx$ hyperfine splitting. Again the results indicate that the hyperfine splitting sets the temporal scale of the experiment.

In Fig. 6 we show the effect of K on the apparent order for the case $\beta = 2.6(\sigma_z = -0.25)$. The curves indicate that σ_z is affected only in the second significant figure: a decrease in K results in an increase in σ_z. In the case $K = 0$, which is not shown, the apparent and real order are the same in the fast tumbling regime. In Fig. 7 we show the effect of K upon the peak to peak linewidth. Here again the effects are small.

In Fig. 8, we show calculated spectra of the $m_I = \pm 7/2$ lines for $K = 2$, $1/\tau = 1.4 \times 10^7\,\mathrm{sec}^{-1}$ (5 G) and $\beta = 2(\sigma_z = -0.21)$, $3.6(\sigma_z = -0.30)$, $7.5(\sigma_z = -0.40)$ and $15(\sigma_z = -0.45)$. This case corresponds to slow tumbling regime and the spectra are all equally contracted. Hence, as shown in Fig. 4, varying the order does not vary the separation here. The spectrum for $\beta = 15$ is symmetric while that

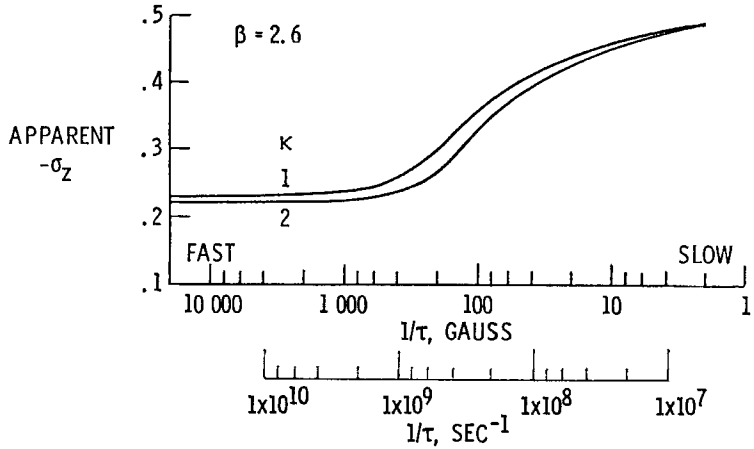

Figure 6. The apparent order, as calculated from the average line separation, versus the tumbling rate, with K as a parameter.

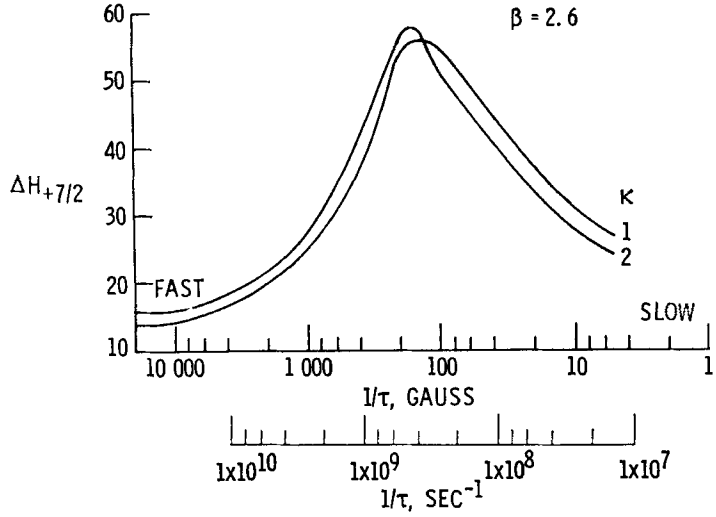

Figure 7. The peak to peak derivative line width of the $m_I = +7/2$ line versus the tumbling rate.

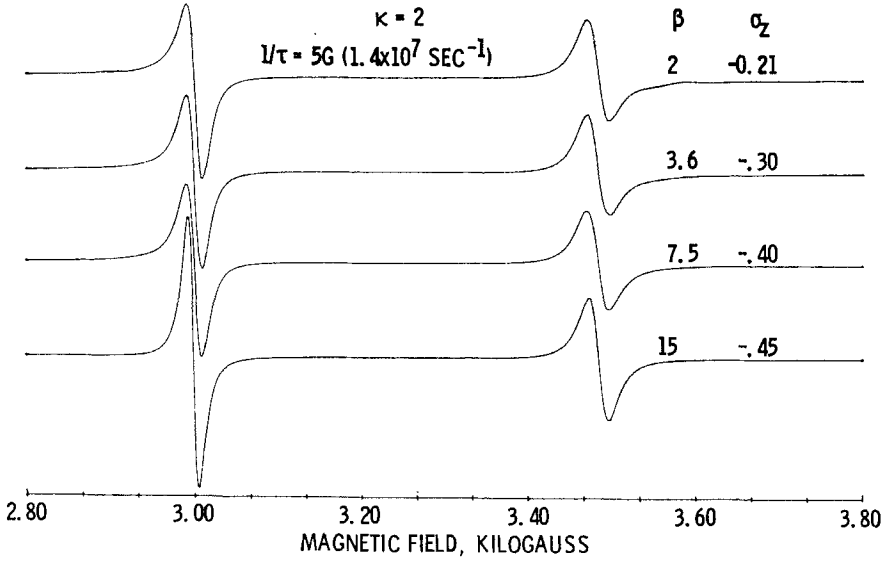

Figure 8. Calculated spectra for different values of the Saupe factor, β, for the case in which the tumbling of the probe is severely inhibited.

for $\beta = 2$ is asymmetric. We define an asymmetry parameter for the $m_I = -7/2$'s line as the amplitude of the low field side divided by the high field side. This parameter is plotted versus β in Fig. 9. The asymmetry parameter increases linearly towards one (no asymmetry). The asymmetry is no longer present for $\beta \gtrsim 10$.

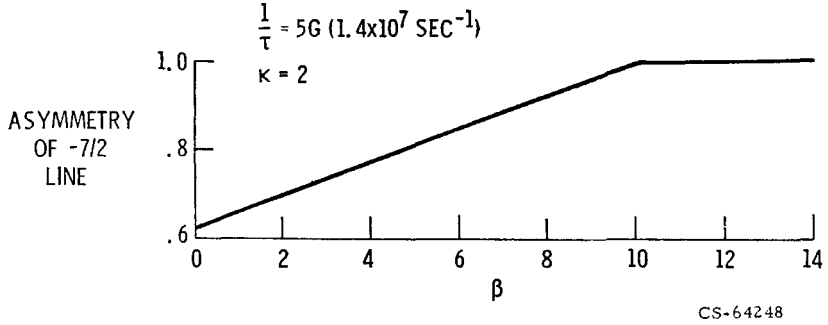

Figure 9. Asymmetry factor versus the Saupe factor, β for the $m_I = -7/2$ line.

In summary, our calculations show that the usual method of calculating the order in a liquid crystal fails when the tumbling rate of the paramagnetic probe is comparable to or less than the hyperfine splitting. Our calculations of apparent order and line shapes versus $1/\tau$ should enable us to determine the order and tumbling times for those cases in which the more conventional method fails. These calculations are useful for both liquid crystals and isotropic liquids ($\beta = K = 0$), and allow one to interpret EPR data in a tumbling time regime which was formally inaccessible to theoretical interpretation.

Acknowledgements

The author (E.G.) would like to acknowledge support from AFOSR under contract F44620-69-C-0021 and the NSF under contract GH-34164X, and the author (J.K.) would like to acknowledge support from the Office of Naval Research under Contract No. N00014-69-C-0218.

Appendix

In the case of large (α, a) and small (b, Δg) we need only deal with the ϕ independent Hamiltonian as given in Eq. (2). If this is not

the case we must consider the so-called secular term

$$\mathscr{H}_2 = \gamma(\theta)\, S_z[I_+ \exp(-i\phi) + I_- \exp(i\phi)]\,, \qquad \text{A-1}$$

where $\gamma(\theta) = (b/2) \sin\theta \cos\theta$.

The density matrix equation, for example, for the isotropic liquid is now

$$\dot{\rho} = -ih^{-1}[\mathscr{H}_0 + \mathscr{H}_1 + \mathscr{H}_2, \rho] + \frac{D}{\sin\theta}\frac{\partial}{\partial\theta}\sin\theta\frac{\partial\rho}{\partial\theta} \qquad \text{A-2}$$

$$+ \frac{D}{\sin^2\theta}\frac{\partial^2\rho}{\partial\phi^2} - \rho/T_2.$$

Perform the unitary transformation

$$\bar{\rho} = \exp(i\mathscr{S})\rho\exp(-i\mathscr{S}), \qquad \text{A-3}$$

to obtain

$$\dot{\bar{\rho}} = -ih^{-1}[\bar{\mathscr{H}}, \bar{\rho}] + \text{the relaxation term in } \bar{\rho}. \qquad \text{A-4}$$

Here

$$\bar{\mathscr{H}} = \exp(i\mathscr{S})\mathscr{H}\exp(-i\mathscr{S}) = \mathscr{H} + i[\mathscr{S}, \mathscr{H}]$$

$$- 1/2[\mathscr{S}, [\mathscr{S}, \mathscr{H}]] + \ldots. \qquad \text{A-5}$$

We chose S such that

$$\mathscr{H}_2 + i[\mathscr{S}, \mathscr{H}_{OD}] = 0, \qquad \text{A-6}$$

where

$$\mathscr{H}_{OD} \equiv \alpha S_z + A(\theta) I_z S_z. \qquad \text{A-7}$$

Then

$$S = -\int_{\omega\to 0}^{0}\exp(i\mathscr{H})OD^t\mathscr{H}_2\exp(-i\mathscr{H})OD^t\exp(-\omega t)\,dt. \qquad \text{A-8}$$

Using standard operator algebra one calculates

$$\mathscr{S} = -i\frac{4\gamma(\theta)}{A(\theta)}S_z(I_+\exp[-i\phi] - I_-\exp[i\phi]). \qquad \text{A-9}$$

Substituting S into

$$\bar{\mathscr{H}} = \mathscr{H}_0 + \mathscr{H}_i + i/2[\mathscr{S}, \mathscr{H}_2] + \ldots \qquad \text{A-10}$$

one obtains (excluding higher order terms)

$$\bar{\mathscr{H}} = \mathscr{H}_0 + \frac{2\gamma(\theta)^2}{A(\theta)} I_z + \omega_1 \tilde{S}_x \cos\omega t, \qquad \text{A-11}$$

where

$$\bar{S}_x = S_x + i[\mathscr{S}, S_x] + \ldots$$

$$= S_x + i\frac{4\gamma(\theta)}{A(\theta)} S_y[I_+ \exp(-i\phi) - I_- \exp(i\phi)]. \qquad \text{A–12}$$

For the linear response solution we set $\bar{\rho} = \bar{\rho}_0 + \bar{\rho}_1$ to obtain from A–4

$$\dot{\bar{\rho}}_1 = -ih^{-1}\left[\mathscr{H}_0 + \frac{2\gamma^2(\theta)}{A(\theta)} I_z, \rho_1\right]$$

$$- i\omega_1 \cos\omega t\left[S_x + i\frac{4\gamma(\theta)}{A(\theta)} S_y(I_+ \exp[-i\phi] - I_- \exp[i\phi]), \bar{\rho}_0\right]$$

$$+ \text{relaxation terms in } \bar{\rho}. \qquad \text{A–13}$$

The solution for $\bar{\rho}_1$ can be written as

$$\rho_1 = \bar{\rho}_1{}^0 + \bar{\rho}_1{}^+ \exp(i\phi) + \bar{\rho}_1{}^- \exp(-i\phi) \qquad \text{A–14}$$

where

$$\dot{\bar{\rho}}_1{}^0 = -ih^{-1}\left[\mathscr{H}_0 + \frac{2\gamma^2(\theta)}{A(\theta)} I_z, \bar{\rho}_1{}^0\right]$$

$$+ \frac{D}{\sin\theta}\frac{\partial}{\partial\theta}\left(\sin\theta \frac{\partial\bar{\rho}_1{}^0}{\partial\theta}\right) - \bar{\rho}_1{}^0/T_2$$

$$- i\omega_1 \cos\omega t[S_x, \rho_0], \qquad \text{A–15}$$

and

$$\dot{\bar{\rho}}_1{}^{\pm} = \frac{D}{\sin\theta}\frac{\partial}{\partial\theta}\left(\sin\theta \frac{\partial\bar{\rho}_1{}^{\pm}}{\partial\theta}\right) - \frac{D}{\sin^2\theta}\bar{\rho}_1{}^{\pm} - \bar{\rho}_1{}^{\pm}/T_2$$

$$\mp \frac{4\gamma(\theta)\omega_1}{A(\theta)}\left[S_y I_{\mp}, \rho_0\right]. \qquad \text{A–16}$$

The $\bar{\rho}_1{}^{\pm}$ solutions have no resonance behavior and thus will contribute a constant background over the entire spectra. Thus they can be ignored. Now we need to calculate

$$M_x = \text{Tr}\,\rho S_x = \text{Tr}\,\bar{\rho}_1\bar{S}_x \approx \text{Tr}\,\bar{\rho}_1{}^0\bar{S}_x$$

$$= \text{Tr}\,\bar{\rho}_1{}^0\left\{S_x + i\frac{4\gamma(\theta)}{A(\theta)} S_y(I_+ \exp[-i\phi] - I_- \exp[i\phi])\right\}.$$

Hence we have exhibited the lowest order ϕ dependent correction to the line shape using the solution to a density matrix equation (A–15) which is formally equivalent to the one for a ϕ independent Hamiltonian.

REFERENCES

1. Glarum, S. H. and Marshall, J. H., *J. Chem. Phys.* **46,** 55 (1967).
2. Chen, D. H. and Luckhurst, G. R., *Trans. Faraday Soc.* **65,** 656 (1969)
3 Schwerdtfeger, C. F. and Diehl, P., *Mol. Phys.* **17,** 417 (1969).
4. Fryburg, G. C. and Gelerinter, E., *J. Chem. Phys.* **52,** 3378 (1970), and NASA TN D-5659 (1970).
5. Goldman, S. A. *et al.*, *J. Chem. Phys.* **56,** 716 (1972).
6. Wilson, R. and Kivelson, D., *J. Chem. Phys.* **44,** 154 (1966).